Journal of the European Ceramic Society 21 (2001) 555–560

www.elsevier.com/locate/jeurceramsoc

TG-DTA study of mixed conductor $Sr_4(Fe_{1-x}Co_x)_6O_{13\pm\delta}$ in air and argon

Takeshi Tsuchida *, Takahiro Kan

Division of Materials Science and Engineering, Graduate School of Engineering, Hokkaido University, North 13 West 8, Kita-ku, Sapporo, 060-8628 Japan

Received 25 May 2000; accepted 15 July 2000

Abstract

The synthesis, structure, electrical conductivity and TG-DTA behavior in air and argon of the $Sr_4(Fe_{1-x}Co_x)_6O_{13\pm\delta}$ samples with $x=0$–0.417 were investigated. While the $Sr_4(Fe_{1-x}Co_x)_6O_{13\pm\delta}$ solid solutions being isostructural with $Sr_4Fe_6O_{13}$ were formed for $0<x\leqslant 0.25$, the $Sr_4(Fe_{1-x}Co_x)_6O_{13\pm\delta}$ phase and the perovskite phase $Sr(Fe_{1-y}Co_y)O_3$ coexisted for $x=0.333$ and the perovskite phases of $Sr(Fe_{1-y}Co_y)O_3$ and $SrCoO_{2.8}$ were formed along with a trace of CoO for $x=0.417$. The total conductivity increased with increasing Co substitution and temperature. The relationship between the weight changes observed in TG experiments and the total conductivity is reported.

Keywords: Batteries; Electrical conductivity; Mixed conductor; Perovskites; Powders-solid state reaction; $Sr_4(Fe,Co)_6O_{13}$

1. Introduction

The mixed-conducting oxides with both oxide-ion and electronic conductivity have received increased attention because of their potential uses as electrodes in solid-oxide fuel cells, batteries, sensors and oxygen separation membranes. Recently, Ma et al.[1–3] have reported that the $SrFeCo_{05}O_x$ oxide exhibits mixed high electronic and oxide-ion conductivity. It shows not only total and ionic conductivity of 17 and 7 S cm^{-1}, respectively, in air at 800°C, but also high oxygen permeability, which are superior to those of yttrium-stabilized zirconia. In addition, this oxide is structurally stable in both oxidizing and reducing atmospheres. Despite its attractive properties, however, the reproducibility of such a high oxide-ion conductivity does not seem to have been confirmed. The structure of $SrFeCo_{05}O_x$ has been studied by Ma et al.[4] and Fjellvag et al.[5] and elucidated on the basis of the perovskite-related structure being isostructural with $Sr_4Fe_6O_{13}$, hence the composition of $SrFeCo_{0.5}O_x$ can be described as $Sr_4(Fe_{1-x}Co_x)_6O_{13\pm\delta}$ with $x=0.333$. Guggilla et al.[6,7] have investigated the various cationic substitutions in both Sr and Fe sites of $Sr_4Fe_6O_{13}$ and the total conductivity of the resulting $Sr_{4-x}Ca_xFe_{6-y}Co_yO_{13+\delta}$.

In this study, in order to get more information on the mechanism of high oxide-ion conduction we have investigated the relationship between synthesis, structure and electrical conductivity of $Sr_4(Fe_{1-x}Co_x)_6O_{13\pm\delta}$ with different substitutions of Fe by Co, and its TG-DTA behaviors in air and argon atmospheres.

2. Experimental procedures

The $Sr_4(Fe_{1-x}Co_x)_6O_{13\pm\delta}$ samples with $x=0$, 0.087, 0.167, 0.200, 0.250, 0.333 and 0.417 were prepared by a solid-state reaction with appropriate amounts of $SrCO_3$(Kojundo Chemical), Fe_2O_3 and $Co(NO_3)_2{\cdot}6H_2O$ (Kanto Chemicals). These starting materials were mixed in required ratios using an agate mortar and a pestle in ethanol, dried and then pressed under a load of 1000 kg cm^2 into a pellet of 10 mm in diameter and 20 mm thick by CIP method. After calcined in air at 850°C for 16 h, the pellet was ground into the powders, pressed again into a pellet and then sintered in air at 1185°C for 5 h. The sintered products were required to have more than 90% of the theoretical density ($\rho=4.99$ g cm^{-3})[3] of $Sr_4(Fe_{1-x}Co_x)_6O_{13\pm\delta}$. The bars ca. $2\times2\times10$ mm^3 were cut from the sintered samples and subjected to optical

* Corresponding author. Tel.: +81-11-706-6578; fax: +81-11-706-6578.

E-mail address: tsuchida@eng.hokudai.ac.jp (T. Tsuchida).

0955-2219/01/$ - see front matter
PII: S0955-2219(00)00215-6

microscopic observations after polishing with 1 μm-diamond paste and etching with a hot HC1 solution, and conductivity measurements. Total conductivity was measured in air and argon atmospheres using a four-probe technique. Platinum wires were attached to the bar with platinum paste (Tokuriki) to serve as current and voltage leads and heated in air at 1000°C. In addition, the bars were ground into powders and subjected to X-ray diffraction (XRD) with a RINT-1.300 (Rigaku Denki) using Fe-filtered CoK_α radiation and TG-DTA measurements at a heating rate of 10°C mm^{-1} in a static air and a flowing argon of 30 ml min^{-1} in a TG-DTA-2000 apparatus (Mac Science).

3. Results and discussion

Fig. 1 shows the XRD patterns of the $Sr_4(Fe_{1-x}Co_x)_6O_{13\pm\delta}$ samples with $x=0$–0.417 sintered at 1185°C in air. The XRD pattern of the sample with $x=0$ agreed completely with that of $Sr_4Fe_6O_{13}$ reported by Kanamaru et al.[8] and no evidence for any secondary phases was found in this sample, indicating that this is a pure phase sample. The samples with $x=0.087$, 0.167, 0.200 and 0.250 show the same as the XRD pattern of the Co-free $Sr_4Fe_6O_{13}$ sample, though the shifts in diffraction angle can be seen, indicating the formation of $Sr_4(Fe_{1-x}Co_x)_6O_{13\pm\delta}$ solid solutions. In contrast, the sample of highest cobalt substitution attempted, with $x=0.417$, was found to contain two kinds of perovskite of $Sr(Fe_{1-y}Co_y)O_3$ and $SrCoO_{2.8}$ and a trace of CoO. The sample with $x=0.333$ showed the XRD pattern of $Sr_4(Fe_{1-x}Co_x)_6O_{13\pm\delta}$ coexisted with $Sr(Fe_{1-y}Co_y)O_3$. The substitution of Fe by Co in the structure of $Sr_4(Fe_{1-x}Co_x)_6O_{13\pm\delta}$ leads to changes in unit cell parameters.

Fig. 2 shows the variation of the orthorhombic lattice parameters and cell volume with Co content in $Sr_4(Fe_{1-x}Co_x)_6O_{13\pm\delta}$. The a and c in cell parameters decrease, while the b increases with increasing Co content. The cell volume also decreases monotonously with increasing Co content. The values of the $Sr_4(Fe_{1-x}Co_x)_6O_{13\pm\delta}$ sample with $x=0.333$ deviate from the linear dependence of these parameters on Co content, probably indicating that the solubility limit of Co in $Sr_4(Fe_{1-x}Co_x)_6O_{13\pm\delta}$ is in the range from $x=0.250$ to 0.333.

Fig. 3 shows the variations of total conductivity with temperature for the different $Sr_4(Fe_{1-x}Co_x)_6O_{13\pm\delta}$ samples. While the $Sr_4Fe_6O_{13}$ sample without Co substitution shows the lowest conductivity of 0.08–0.57 S cm^{-1} at 200–1000°C, the conductivities for the $Sr_4(Fe_{1-x}Co_x)_6O_{13\pm\delta}$ samples with $x=0.167$–0.417 increased significantly with increasing Co substitution and temperature. Particularly, the $Sr_4(Fe_{1-x}Co_x)_6O_{13\pm\delta}$ sample with $x=0.417$ showed the highest conductivity of 64.6 S cm^{-1} at 600°C. However, it is considered that the highest conductivity of this sample is related to the perovskite

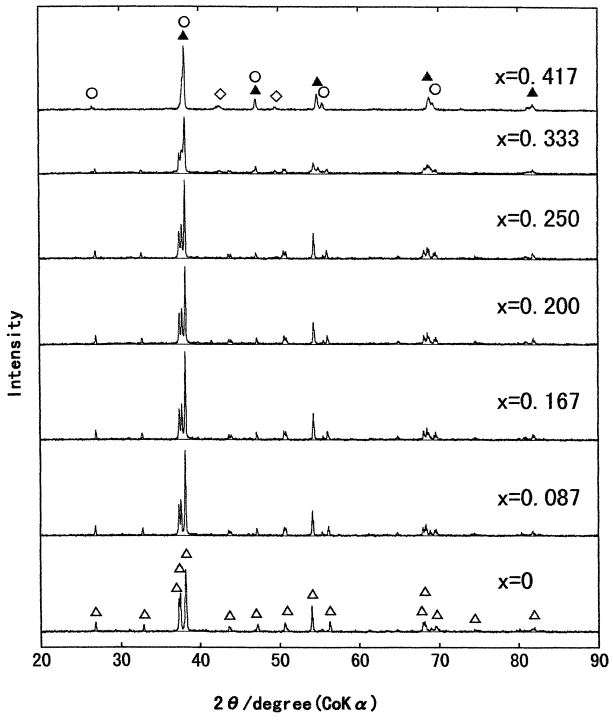

Fig. 1. XRD patterns of the $Sr_4(Fe_{1-x}Co_x)_6O_{13\pm\delta}$ samples with $x=0$–0.417 sintered at 1185°C in air. △: $Sr_4Fe_6O_{13}$, ▲: $Sr(Fe_{1-y}Co_y)O_3$, ○: $SrCoO_{2.8}$, ◇: CoO.

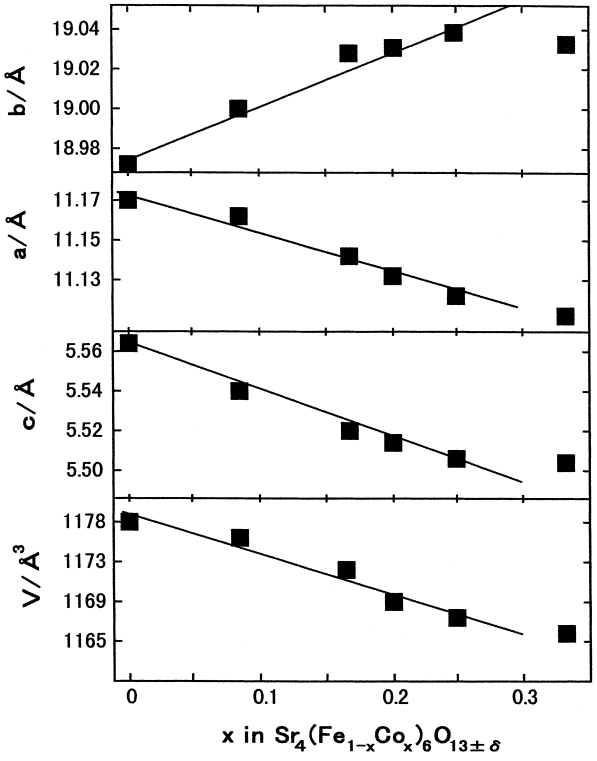

Fig. 2. The variation of the orthorhombic lattice parameters and cell volume with Co content in the $Sr_4(Fe_{1-x}Co_x)_6O_{13\pm\delta}$ samples.

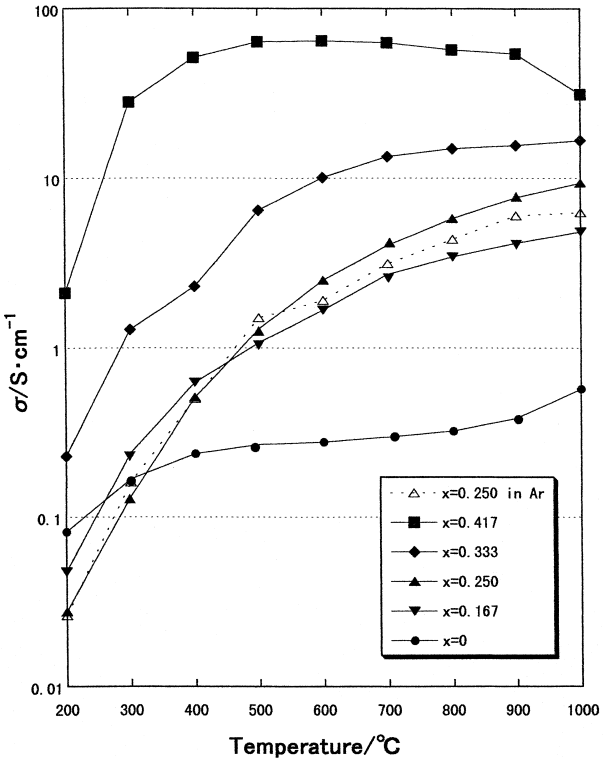

Fig. 3. The variations of total conductivity with temperature for the $Sr_4(Fe_{1-x}Co_x)_6O_{13\pm\delta}$ samples with $x=0$, 0.167, 0.250, 0.333 and 0.417 in air and argon.

phases of $Sr(Fe_{1-y}Co_y)O_3$ and $SrCoO_{2.8}$ formed, as already shown in Fig. 1, because these perovskite phases exhibit much higher electronic conductivity than oxide-ion conductivity.[7,9] In contrast, the conductivity of $Sr_4(Fe_{1-x}Co_x)_6O_{13\pm\delta}$ with $x=0.250$, which is a single phase, was 9.4 and 6.2 S cm^{-1} in air and argon atmospheres at 1000°C, respectively, compared with 20 and 6 S cm^{-1} in air and argon at 900°C for $Sr_4Fe_4Co_2O_{13}$.[4] From the linear dependence plot of the log σ on reciprocal temperature ($1/T$) in air, the activation energies were calculated to be 5.3, 13.5, 15.9 and 13.5 kJ mol^{-1} for $Sr_4Fe_6O_{13}(x=0)$, $Sr_4Fe_5CoO_{13}(x=0.167)$, $Sr_4Fe_{4.5}Co_{1.5}O_{13}(x=0.250)$ and $Sr_4Fe_4Co_2O_{13}$ ($x=0.333$), respectively.

Figs. 4–6 show TG-DTA curves of the $Sr_4(Fe_{1-x}Co_x)_6O_{13\pm\delta}$ samples with $x=0$, 0.250 and 0.333 in a static air and a flowing argon. In contrast to the almost featureless DTA curves, the significant differences in TG curves can be observed. In Fig. 4(a) and (b), the Co-free $Sr_4Fe_6O_{13}$ ($x=0$) sample showed a tiny weight change of only±0.2 wt.% during the heating and cooling runs repeated two times in air or argon. This value seems to be within the experimental error, and therefore it can be suggested that this sample is fully stable up to 1000°C both in oxidizing and reducing atmospheres. In contrast, the $Sr_4Fe_{4.5}Co_{1.5}O_{13}$ ($x=0.250$) sample showed somewhat bigger weight change than that for $Sr_4Fe_6O_{13}$. In air [Fig. 5(a)], the sample showed the weight increase of 0.3 wt.% at 300–500°C and then the decrease of 0.5 wt.% during further heating up to 1000°C. The weight decrease observed during the second heating from 200 to 1000°C was also about 0.4 wt.%. These weight decreases by heating were almost recovered by cooling down to 200°C. In argon [Fig. 5(b)], a tendency of progressive weight loss of 0.5 wt.% appeared for both the first and second heating runs. On the other hand, in Fig. 6(a) and (b) the $Sr_4Fe_4Co_2O_{13}$ ($x=0.333$) sample showed the remarkable weight decreases of 1.3 and 1.5 wt.% during the first heating up to 1000°C in air and argon atmospheres, respectively. However, it is very interesting that these weight losses were recovered almost completely in air and incompletely in argon during cooling down to 200°C. This indicates that the $Sr_4Fe_4Co_2O_{13}$ ($x=0.333$) oxide causes easily a reversible absorption–desorption of oxygen from air, which behavior is well known to be characteristic of the perovskite oxides.

Prior to discussion about the relationship between the total conductivity in Fig. 3 and the behaviors in TG-DTA curves in Figs. 4–6, it is important to understand the structure of $Sr_4(Fe_{1-x}Co_x)_6O_{13\pm\delta}$. As shown in Fig. 1, the XRD patterns of $Sr_4(Fe_{1-x}Co_x)_6O_{13\pm\delta}$ ($0<x\leqslant 0.250$) satisfactorily fitted to that of $Sr_4Fe_6O_{13}$ ($x=0$).[8] According to Guggilla et al.,[7] a perovskite-related phase $Sr_4(Fe_{1-x}Co_x)_6O_{13\pm\delta}$ is isostructural with $Sr_4Fe_6O_{13}$,[8,10] which has a layered intergrowth structure. The perovskite-type SrO–FeO_2–SrO blocks are sandwiched by $Fe_2O_{2.5}$ blocks along the *b*-axis. While the Fe atoms in the perovskite layer have a distorted octahedral coordination with the FeO_6 octahedra sharing corners, those in the Fe_2O_{25} layers have both distorted tetragonal pyramidal and trigonal bipyramidal oxygen coordinations. The FeO_5 trigonal bipyramids share edges among themselves. Similarly, the FeO_5 tetragonal pyramids share edges among themselves. The three types of polyhedra are connected to each other by sharing corners, in which Fe^{3+} cations are present with three different oxygen coordinations. The Co ions can in principle substitute for all the three types of Fe^{3+} cation. However, it is needed to be determined by neutron diffraction study which sites of the three non-equivalent Fe sites are substituted by Co ions or which is the valency of Co ions, Co^{2+} or Co^{3+}. The ionic conductivity in $Sr_4(Fe_{1-x}Co_x)_6O_{13\pm\delta}$ must originate from transport of oxygen ion vacancies or interstitial oxygen. If an Fe^{3+} cation in the FeO_5 trigonal bipyramids or tetragonal pyramids layers is substituted by a Co^{2+} cation, an oxide-ion vacancy is formed. Then, the $Sr_4(Fe_{1-x}Co_x)_6O_{13\pm\delta}$ ($0<\times\leqslant 0.250$) samples has an oxygen-deficient perovskite-related layered structure, and can absorb oxygen in high Po_2 and release oxygen in low Po_2. Hence, the (Fe, Co)$O_{2.5}$ layer in $Sr_4(Fe_{1-x}Co_x)_6O_{13\pm\delta}$ would provide the main conducting paths for the oxide ion transport.

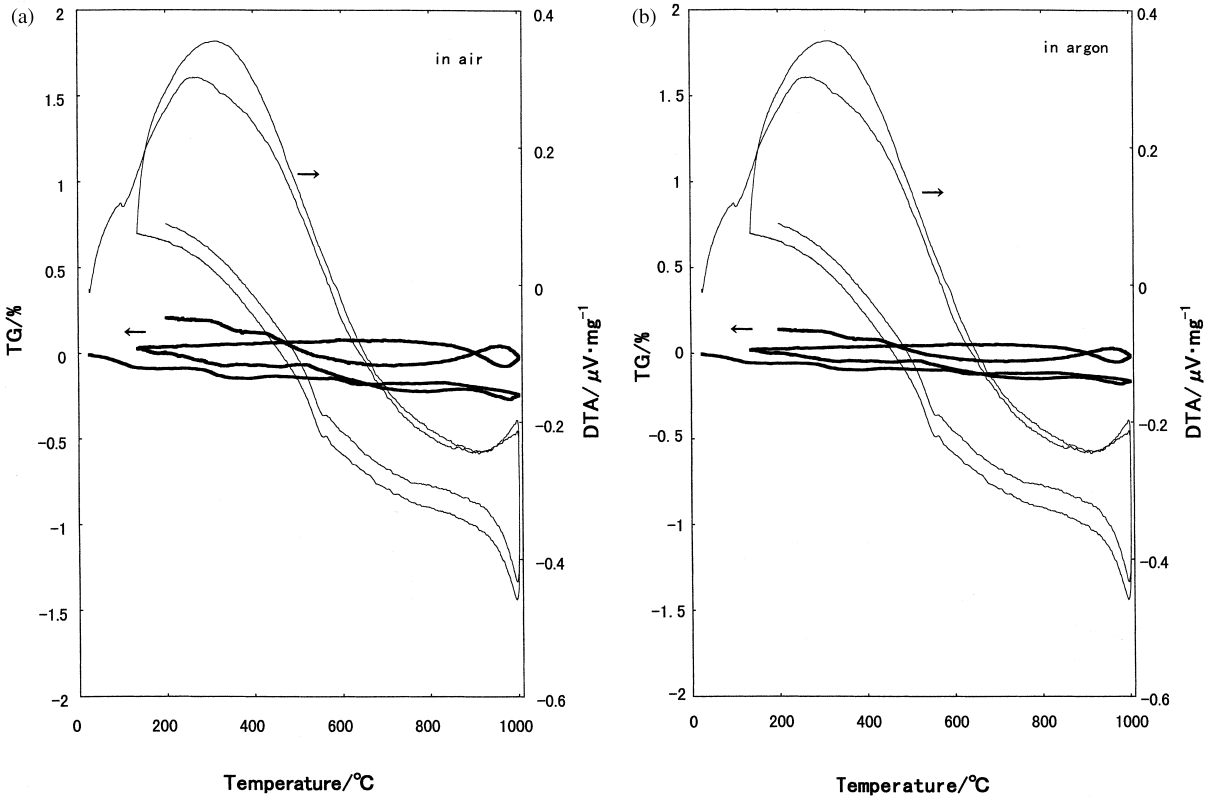

Fig. 4. TG-DTA curves of the $Sr_4Fe_6O_{13}$($x=0$) sample in (a) a static air and (b) a flowing argon.

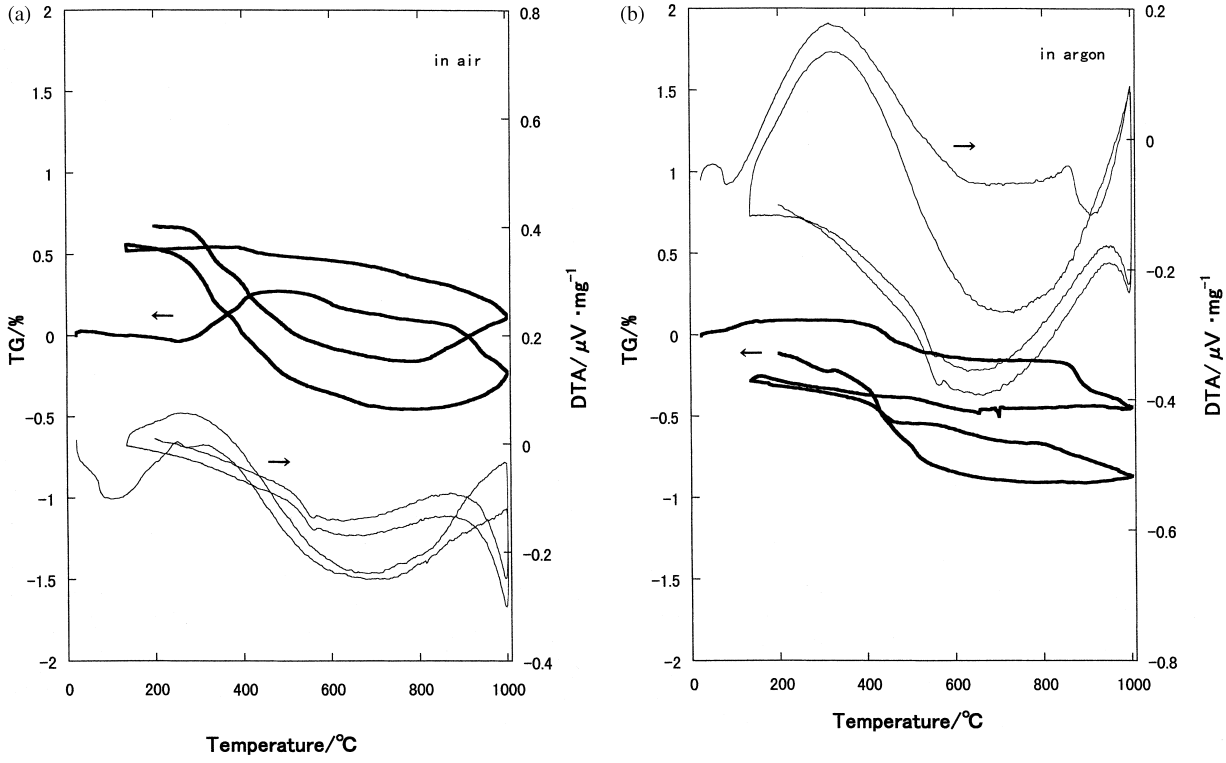

Fig. 5. TG-DTA curves of the $Sr_4Fe_{4.5}Co_{1.5}O_{13}$($x=0.250$) sample in (a) a static air and (b) a flowing argon.

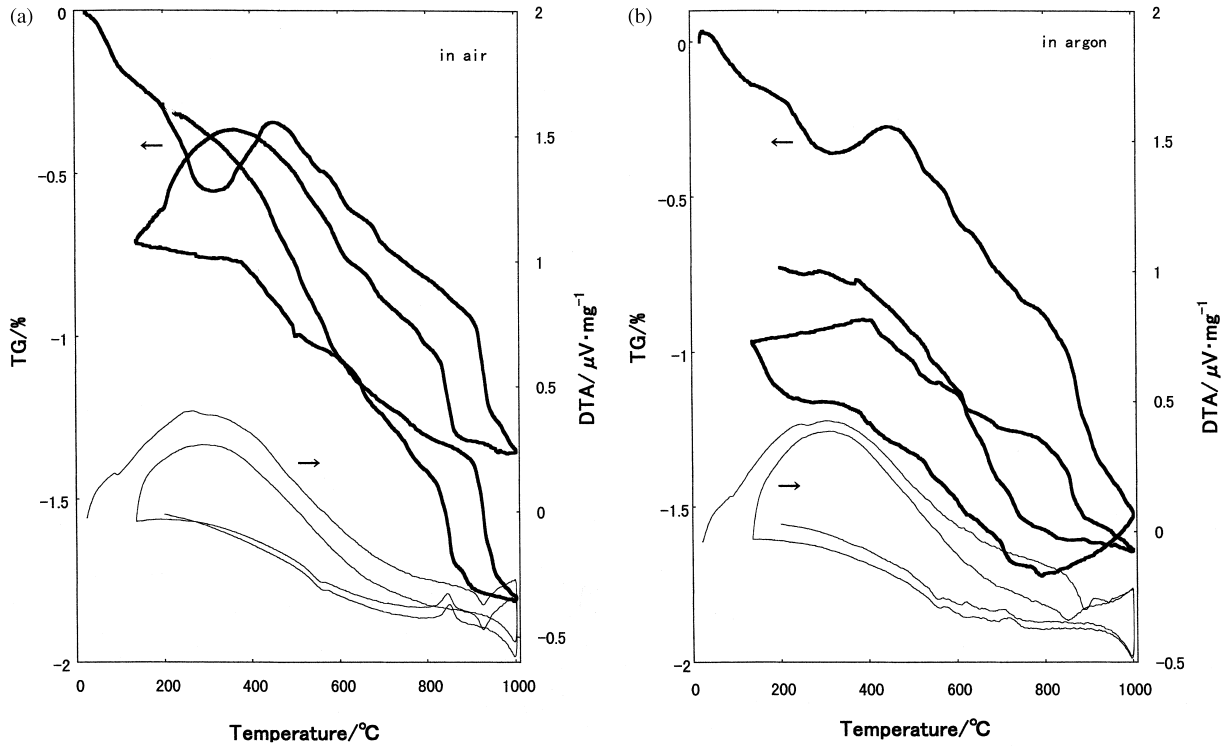

Fig. 6. TG-DTA curves of the $Sr_4Fe_4Co_2O_{13}$($x=0.333$) sample in (a) a static air and (b) a flowing argon.

In our results shown in Fig. 5(a), the $Sr_4Fe_{4.5}Co_{1.5}O_{13}$($x=0.250$) sample showed a very small weight increase of 0.3 wt.% at 300–500°C and then the decrease of 0.5 wt.%, as a whole, on further heating up to 1000°C. Although this relatively small weight decrease clearly differs from the big one (1.3 wt.%) for $Sr_4Fe_4Co_2O_{13}$($x=0.333$) shown in Fig. 6(a), it can be estimated that the ionic conductivity of the $Sr_4Fe_{4.5}Co_{1.5}O_{13}$($x=0.250$) sample is led by oxygen-ion vacancy mechanism. However, the measurements of ionic conductivity as a function of oxygen partial pressure showed that the oxide-ion conduction occurs by interstitial oxide ions in $Sr_4(Fe_{1-x}Co_x)_6O_{13\pm\delta}$, because it has been observed that the ionic conductivity increased when the ambient oxygen partial pressure increased.[1] In addition, according to Guggilla et al.,[6] the composition of the $Sr_4Fe_{4.5}Co_{1.5}O_{13}$ ($x=0.250$) sample was estimated to be nearly stoichiometric without oxygen vacancies from oxygen analysis by iodometric titration. Therefore, they also suggested that the oxide-ion conduction in the $Sr_4(Fe_{1-x}Co_x)_6O_{13\pm\delta}$ oxide occurs by the interstitial mechanism. Then the five coordinated Fe^{3+} (or Co^{3+}) ions can assist the oxygen transport via interstitial mechanism by readily adopting sixfold coordination and increasing the formal valence to Fe^{4+} or Co^{4+}. Thus, it seems to be very complicated to explain the relationship between the weight changes shown in Fig. 5(a) and (b) and the interstitial mechanism reported previously[1,6] and therefore further study is needed.

On the other hand, as shown in Fig. 6(a) and (b), the $Sr_4Fe_4Co_2O_{13}$($x=0.333$) sample showed the big weight losses of 1.3 and 1.5 wt.% in air and argon on first heating, which is probably by the loss of oxygen atom from the structure, resulting in the formation of oxygen vacancy. As shown in Fig. 1, this sample is not a single phase material, but consists of the mixture of the $Sr_4Fe_4Co_2O_{13}$ phase and the perovskite phase $SrFeO_{3-\delta}$. Therefore, the increased concentration of oxygen vacancies in the perovskite phase $SrFeO_{3-\delta}$ by heating can decisively contribute to an increase in total conductivity. In fact, it is well known that the perovskite oxides easily tend to lose oxygen at higher temperature or under reducing conditions. However, the perovskites generally have a high electronic component, despite a high total conductivity. Therefore, it is considered that in our sample the contribution of the oxide-ion conductivity to the total conductivity, i.e. ionic transference number, is not so big.

The substitutions of Fe in $Sr_4(Fe_{1-x}M_x)_6O_{13\pm\delta}$ by M = Mn, Ni and Cu ($x=0.250$) have also been attempted. Unfortunately, the $Sr_4(Fe_{1-x}M_x)_6O_{13\pm\delta}$ phase was not formed, but the $Sr(Fe_{1-y}Co_y)O_3$ perovskite phase was formed.

References

1. Ma, B., Balachandran, U. and Park, J. H., Electrical transport properties and defect structure of $SrFeCo_{0.5}O_x$. *J. Electrochem. Soc.*, 1996, **143**(5), 1736–1744.
2. Ma, B., Park, J. H. and Balachandran, U., Analysis of oxygen transport and stoichiometry in mixed-conducting $SrFeCo_{0.5}O_x$ by conductivity and thermogravimetric analysis. *J. Electrochem. Soc.*, 1997, **144**(8), 2816–2823.

3. Ma, B. and Balachandran, U., Oxygen nonstoichiometry in mixed-conducting $SrFeCo_{0.5}O_x$. *Solid State Ionics*, 1997, **100**, 53–62.
4. Ma, B., Hodges, J. P., Jorgensen, J. D., Miller, D. J., Richardson, J. W. Jr and Balachandran, U., Structure and property relationships in mixed-conducting $Sr_4(Fe_{1-x}Co_x)_6O_{13\pm\delta}$ materials. *J. Solid State Chem.*, 1998, **141**, 576–586.
5. Fjellvag, H., Hauback, B. C. and Bredesen, R., Crystal structure of mixed conductor $Sr_4Fe_4Co_2O_{13}$. *J. Mater. Chem.*, 1997, **7**(12), 2415–2419.
6. Guggilla, S. and Manthiram, A., Crystal chemical characterization of the mixed conductor $Sr(Fe,Co)_{1.5}O_y$ exhibiting unusually high oxygen permeability. *J. Electrochem. Soc.*, 1997, **144**(5), L120–L122.
7. Guggilla, S., Armstrong, T. and Manthiram, A., Synthesis, crystal chemistry, and electrical properties of the intergrowth oxides $Sr_{4-x}Ca_xFe_{6-y}Co_yO_{13+\delta}$. *J. Solid State Chem.*, 1999, **145**, 260–266.
8. Kanamaru, F., Shimada, M. and Kiozumi, M., Crystallographic properties of and Mossbauer effect in $Sr_4Fe_6O_{13}$. *J. Phys. Chem. Solids*, 1972, **33**, 1169–1171.
9. Taguchi, H., Shimada, M. and Kiozumi, M., The electrical properties of ferromagnetic $SrCoO_{3-\delta}$ ($0 < \delta < 0.5$). *Mater. Res. Bull.*, 1980, **15**, 165–171.
10. Yoshiasa, A., Ueno, K., Kanamaru, F. and Horiuchi, H., Structure of $Sr_4Fe_6O_{13}$, a new perovskite-derivative in the Sr–Fe–O system. *Mater. Res. Bull.*, 1986, **21**, 175–181.